RAINDROP SHAPE-SIZE RELATION RETRIEVAL
FROM POLARIMETRIC RADAR MEASUREMENTS

E. Gorgucci*, L. Baldini, Institute of Atmospheric Sciences and Climate – CNR, Roma, Italy
V. Chandrasekar, Colorado State University, Fort Collins CO 80523

1. INTRODUCTION

This paper presents a technique by which it is possible to retrieve the drop shape-size relation that governs the polarimetric radar observations of reflectivity, Z_h, differential reflectivity Z_{dr}, and specific differential propagation phase K_{dp}. To study the shape–size relation, an observation domain is introduced. In this space, called Radar Drop Shape Size Domain, (RDSSD), the DSD variability is almost eliminated and any variation is essentially due to the drop shape variability, allowing the same to be observed. The RDSSD can be mapped to a corresponding domain in which the drop shape is expressed through the relation between the ratio between the semi-minor axis and the semi-major axis (b and a, respectively) of the oblate spheroid approximating the drop and the equivolumetric diameter of the drop (D). This drop shape-size domain is parameterized with a fourth-order polynomial. A minimization procedure of the error between the measured values of observables and values from a priori model in RDSSD is developed by changing elements of the above-mentioned polynomial. As a result, a relation between the axis ratio b/a and D that approaches the underlying unknown relation governing the prevailing radar measurements is found.

The procedure is applied to three different radar data sets collected by the NCAR S-POL radar during campaigns conducted in different climatic region, namely Florida (Teflun B), Brazil (LBA) and Italy (MAP). The drop shape-size relations obtained for each campaign are compared with relations proposed in the literature. The mean drop shape-size relation retrieved is analyzed to explore whether the natural raindrop shape-size relation can be described by a unique model.

2. THE RADAR DROP SHAPE-SIZE DOMAIN

The radar measurements Z_h, Z_{dr}, and K_{dp} are all influenced by the DSD variability and by the raindrop shape-size relation. It has been long established that Z_{dr} is mostly sensitive to drop median volume diameter (D_0) and to raindrop shape, whereas K_{dp} is mostly sensitive

to concentration and shape. Gorgucci et al. (2006) showed that by collapsing the self-consistency principle onto a two-dimensional space defined by the two variables K_{dp}/Z_h and Z_{dr}, the influence of DSD is nullified so that any variation in this domain comes predominantly from the drop shape variability. The ratio between K_{dp} and Z_h will be henceforth referred to with $\chi_{pp}=10\log_{10}(K_{dp}/Z_h)$, where K_{dp} is in units of deg km^{-1} and Z_h in m^3 mm^{-6}. The space defined by the two variables χ_{pp} and Z_{dr} (in dB) is called the "Radar Drop Shape-Size Domain" (RDSSD) because it allows one to obtain drop shape information directly from radar observations. The position of a (χ_{pp}, Z_{dr}) pair in the RDSSD is determined by the prevailing shape-size of the drops contained in the radar measurement volume.

To study the raindrop shape–size variability in the RDSSD, the averaged χ_{pp}–Z_{dr} relations can be drawn for commonly used raindrop shape models available in the literature. A simulation procedure was built using the following conditions: i) gamma DSD parameters varying in the range defined by $0.5<D_0<3.5$ mm; $3<\log_{10}N_w<5$; $-1<\mu<5$; ii) $10\log_{10}Z_h<55$ dBZ iii) rain rate less than 300 mm h^{-1}; iv) drops canted with the mean and standard deviation equal to 0° and 10°, respectively. In this study, the shape-size relations of Pruppacher and Beard (1970), Beard and Chuang (1987) as well as the two recent ones of Brandes et al. (2002) and Thurai et al. (2007) are considered. Hereinafter, these relations will be referred to as PB, BC, BZV, and THBRS, respectively.

Figure 1 compares χ_{pp} versus Z_{dr} for these models using results from the simulation described above. It can be seen that in the RDSSD most of the variability resulting from DSD has been eliminated and each drop shape–size model can be easily recognized. Therefore using polarimetric radar measurements, a domain that is essentially sensitive to raindrop shape has been created.

3. DROP SHAPE RETRIEVAL PROCEDURE

With the exception of the relation of PB that is linear, the other equations are expressed by forth order polynomials. For this reason, we attempt to retrieve the shape-size relation underlying polarimetric radar measurements in term of a fourth order polynomial. The procedure for retrieving the mean drop shape from radar measurements consists of the following steps:

* Corresponding author address: Eugenio Gorgucci, ISAC-CNR, Via Fosso del Cavaliere, 100, 00133 Roma, Italy; e-mail: e.gorgucci@isac.cnr.it
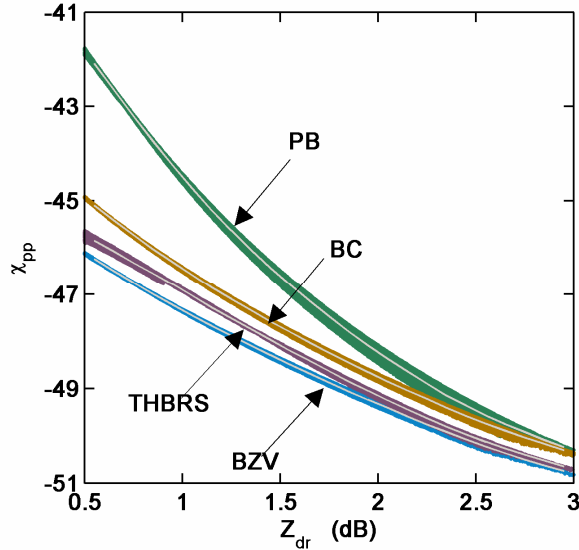
Figure 1. Scatter plot of χ_{pp} as a function of Z_{dr} for widely varying DSD and the drop shape-size relations of PB, BC, THBRS, and BZV. Grey solid lines represent averaged χ_{pp} as a function of Z_{dr}.

a) 20000 triplets {N_w, D_0, μ}, in the intervals defined in sect. 2 are generated.
b) A fourth-order polynomial equation is chosen to describe the axis ratio-diameter relation.
c) For each DSD triplet, radar measurements are simulated assuming the fourth order polynomial set at step b) to obtain a corresponding set of (χ_{pp}, Z_{dr}) pairs.
d) Z_{dr} is stratified in classes of 0.1 dB and the mean values of χ_{pp} are computed for each class
e) The square error between mean values of simulated and measured χ_{pp} is computed for each Z_{dr} class.
f) The root mean square error (RMSE) is computed over all the radar data.
g) The minimization of the RMSE is obtained by changing the coefficients of the fourth-order polynomial equation of the drop shape-size relation.

To find the starting fourth-order polynomial, the plane describing the relation between the drop axial ratio b/a and the drop diameter D is divided in four regions bounded between the D values of 0-2 mm, 2-4 mm, 4-6 mm, and 6-8 mm, respectively. In the first region, a drop is supposed to be spherical up to 0.5 mm. For larger diameters, the axial ratio is described by a curve whose points are at a fixed distance between the PB and BC curves. The distance is defined as a percentage ε of the axial ratio distance between the PB and BC models. Therefore, for ε<50 % the curve lies

closer to the PB model whereas is closer to the BC model for ε>50 %. For ε>100% the curve describes drops that are less oblate than the BC model. In the subsequent regions, the axial drop ratio is described by a piece-wise linear curve whose segments have variable slopes. The fourth order polynomial equation is determined by fitting a fourth-order polynomial to the four segments.

3.1 *Influence of measurement errors on* χ_{pp}

The three polarimetric radar measurements Z_h, Z_{dr}, and K_{dp} are affected by measurement errors that are nearly independent and will directly affect any parameters that are derived from them, like χ_{pp}. Z_h, based on an absolute power measurement, has a typical accuracy of 1 dB, while Z_{dr}, which is a relative power measurement, can be estimated to an accuracy of about 0.2 dB. The accuracy of the K_{dp} estimate depends on the procedure used to compute the range derivative of the the differential propagation phase Φ_{dp} which can be estimated to an accuracy of a few degrees. A least square fit to the Φ_{dp} profile is used to estimate K_{dp}. To ensure that in χ_{pp} computation the measurements come from the same volume, Z_h and Z_{dr} are obtained from power measurements averaged over the path over which K_{dp} is computed. These path measurements can be affected by gradients. Gorgucci et al. (2006) showed that in the occurrence of the DSD variability along the path revealed by the presence of a Z_h gradient, the difference between point- and path-wise values of χ_{pp} and Z_{dr} is negligible.

When Z_{dr} assumes low values, due to signal fluctuation, K_{dp} has a high probability of assuming negative values and therefore χ_{pp} cannot be computed. As a result, for small Z_{dr}, χ_{pp} will be biased to higher values. As the path length decreases, the variance of K_{dp} increases and then the χ_{pp} bias is expected to rise. The sensitivity of χ_{pp} with respect to the path length was studied by Gorgucci et al. (2009) using realistic profiles of DSD parameters simulated from NCAR SPOL radar measurements using the procedure of Chandrasekar et al. (2006). A shift of χ_{pp} toward values higher than those of the theoretical curve model was shown to be evident for small Z_{dr}. Moreover, it increases as the path length decreases. In the case of 15-km path length, for Z_{dr} greater than 0.7 dB, the average value of χ_{pp} practically coincides with the average point-wise χ_{pp}.

3.2 *Bias removal*

In the RDSSD, a bias on Z_{dr} corresponds to a left or right shift along the abscissa, whereas any error on Z_h is directly converted into an up or down shift of χ_{pp}. These

biases will be interpreted in terms of oblateness invalidating the drop-shape retrieval. However, the Z_{dr} bias can be easily removed by several techniques (e.g. Gorgucci et al. 1999; Ryzkhov et al. 2005, Bechini et al. 2008). Techniques based on the self-consistency of polarimetric measurements (Gorgucci et al. 1992) can be used to calibrate Z_h. However, they require an a priori assumption of a fixed drop shape model and uncertainty of this assumption will affected the bias estimate. A different method can be implemented in the RDSSD. For each of the drop shape-size relation considered in this study, the root mean square error between the measured χ_{pp} and the mean χ_{pp} versus Z_{dr} curve of the model was computed for profiles with $Z_{dr}>0.7$ dB (see sect 3.1) varying the Z_h bias. The absolute minimum RMSE provides the mean for knowing which model is closer to the underlying the radar measurements. The corresponding Z_h bias is used to correct the measured radar reflectivity. In fact, in the extreme case that all the experimental χ_{pp} mean values coincide with the corresponding values of the fixed drop shape model, the Z_h bias represents the absolute calibration of the radar system. The method utilized in this study to find the radar calibration bias is conceptually more accurate than the one based on the self consistency of the polarimetric measurements. Once the Z_h bias is found, also the mean shape can be found as described before. This shape, in turn, will provide a slightly different bias in Z_h such that the whole process converges In this way, the method simultaneously determines the mean shape model according to a fourth order polynomial as well as a Z_h bias estimate.

3.3   *Reliability of retrieval*

The estimation error associated with the drop shape retrieval will depend on several factors, namely, Z_h, Z_{dr}, K_{dp} measurement errors, χ_{pp} population size, χ_{pp} population distribution in the RDSSD, reliability of obtaining the fourth-order polynomial by the fitting of a piecewise curve composed of four segments. The procedure to estimate the shape-size relationship was first tested applying it to data simulated assuming a fixed drop shape model (e.g. BC) and verifying the retrieval results. Results showed an excellent agreement (NSE of 3% and negligible NB). To evaluate the impact of measurement errors, a Gaussian noise was added to the curve of mean χ_{pp} for a given shape-size model The standard deviation of the Gaussian noise was chosen to correspond to that of χ_{pp} computed from a sample of 2000 measurements, which can be considered a small percentage of the amount of data that is usually collected by a meteorological radar. It has been shown that the residual region of the difference between the true BC relation and any of those retrieved

is less than 0.002 for D< 3mm and less than 0.01 for 3 < D < 6.5 mm.

4. RESULTS

Radar data used for this study were collected by the NCAR S-POL radar during three campaigns, two of which were conducted as part of the validation program of the Tropical Rainfall Measuring Mission (TRMM), the Texas and Florida Underflight (TEFLUN-B) and the Large Scale Biosphere-Atmosphere (LBA) experiments. The third campaign was the Mesoscale Alpine Programme (MAP) conducted in Europe over the Alpine region. TEFLUN-B was conducted between 1 August and 30 September 1998, in the central region of Florida; the TRMM-LBA campaign took place in Brazil in the Amazonia region from 1 January through 28 February 1999. The MAP experiment was carried out from September to November 1999. The S-POL was located at the southern end of Lake Maggiore, in Italy. Only data collected during the Special Observing Period (SOP) of 19-21 September 2001 are considered.

Profiles of Z_h, Z_{dr}, and Φ_{dp} were selected based on the requirement that they refer to a rain path of over 100 consecutive 0.15-km range bins. This condition was verified using appropriate threshold values of correlation coefficient, received power, reflectivity factor, and standard deviations of Z_{dr} and Φ_{dp} (computed using a 5-range-bin moving window). Moreover, the increase of Φ_{dp} had to be greater than 6 degrees. The procedure described in sect 3.2 was applied to correct the bias in Z_h.

Fig. 2a shows the RDSSD for the data set extracted from the TEFLUN-B campaign. The solid black line with circles represents the mean χ_{pp} vs. Z_{dr} of experimental data. The curve corresponding to the solid red line represents in the RDSSD the retrieved fourth-order polynomial shape-size equation retrieved, that is

$$\frac{b}{a} = 0.999 + 3.131 \times 10^{-2} D - 4.437 \times 10^{-2} D^2 \quad (1)$$
$$+ 7.425 \times 10^{-3} D^3 - 4.157 \times 10^{-4} D^4$$

Also shown are the curves referring to PB, BC, BZV, and THBRS models. The polynomial (1) results from a curve characterized by an ε=170% in the region 0<D<2 mm yielding drops that are less oblate than the BC model. In fact, it is very close to the BZV up to D=6 mm and, for larger diameters, presents an increasing oblateness.

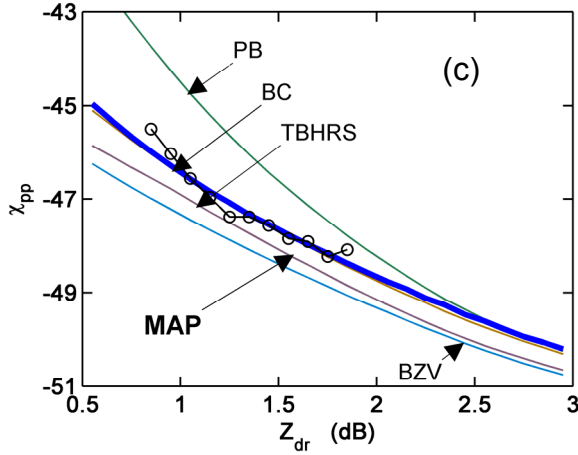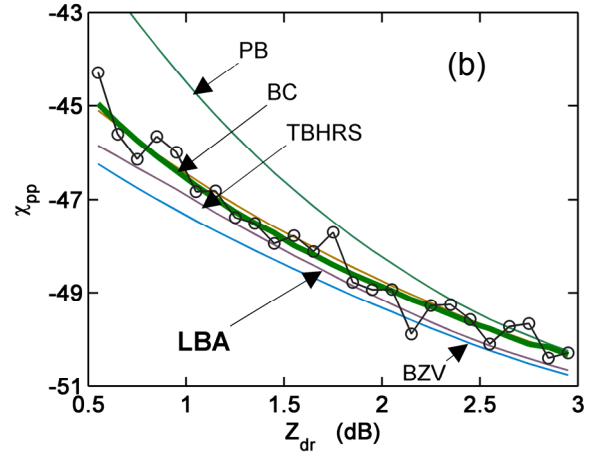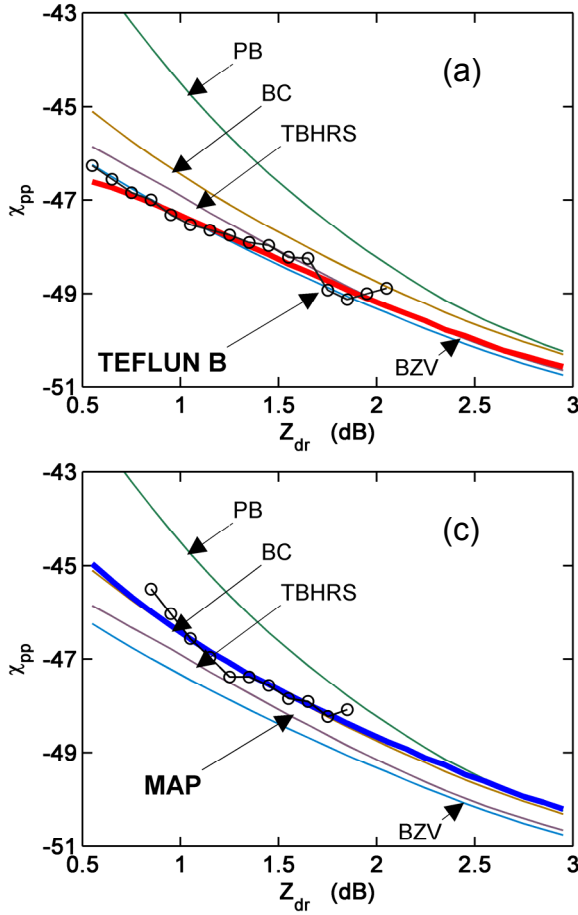The RDSSD obtained using the profiles selcted from the TRMM-LBA campaign is shown in Fig. 2b.

Figure 2. RDSSD for the data collected during the TEFLUN-B (a), LBA (b), and MAP (c) campaigns. PB, BC, BZV, THBRS mean curves are also reported as reference. The solid black lines with circles represent, for each Z_{dr} class of 0.1 dB, the experimental mean value of χ_{pp}. Solid thick lines (red, green, and blue, for TEFLUN B, LBA, and MAP, respectively) represent the fourth-order polynomial equation expressing the retrieved shape-size relations in the RDSSD.

Estimation of the underlying drop shape-size relation is obtained as

$$\frac{b}{a} = 1.009 - 1.207 \times 10^{-2} D - 1.688 \times 10^{-2} D^2 \qquad (2)$$
$$+ 1.467 \times 10^{-3} D^3 - 1.266 \times 10^{-5} D^4$$

Eq. (2) results from a curve characterized by ε=110% in the first region. This means that the LBA drop shape-size relation is close to the BC model but drops are slightly less oblate. This behaviour holds up to D=4 mm. After that drops become more oblate than BC, with increasing values of b/a up to D=6.5 mm after decreasing up to join with BC for D=8 mm.

The mean experimental χ_{pp} curve obtained form the MAP SOP of 19-21 September 2001, is shown in Fig. 2b (black line with markers). For Z_{dr} ranging between 1 and 1.4 dB, it presents two slopes. This behaviour may be due to the presence of wet hail that increases Z_h in

the presence of low Z_{dr}. The retrieved drop shape-size, represented by a thick solid blue line in Fig. 3c is

$$\frac{b}{a} = 1.008 - 6.705 \times 10^{-3} D - 2.009 \times 10^{-2} D^2 \qquad (3)$$
$$+ 1.829 \times 10^{-3} D^3 - 9.270 \times 10^{-6} D^4$$

It must be pointed out that (3) results from a curve with ε=110% in the first region. In fact, up to D=3.5, (3) is superimposed onto the BC and for greater D presents axial ratio values lower than all the other relations. For D>7 mm and D=8 mm, the axial ratio remains almost constant. The comparison of the MAP with the LBA drop axial ratio shows that the two curves are very close except for D>6 mm, where MAP presents values higher than LBA.

The ability of each model to represent the experimental data is analyzed in terms of NSE and NB computed between the experimental χ_{pp} values obtained
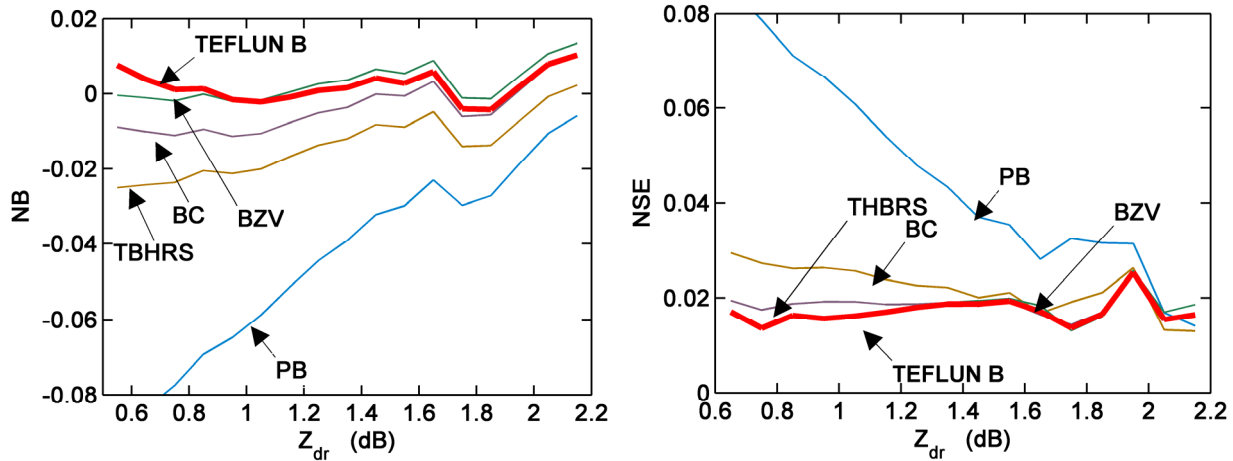
Figure 3. NB (left) and NSE (right) between χ_{pp} values obtained from TEFLUN-B radar data and the corresponding ones of the PB, BC, BZV, THBRS, and polynomial (2) model, respectively. NB and NSE are normalized to the mean χ_{pp} radar data.

experimentally by radar measurements and the corresponding mean value obtained by a fixed model normalized with respect to the mean value of the model and by the corresponding NB. NSE and NB are plotted as a function of Z_{dr} in Fig 3 for the TEFLUN B dataset. NB presents a value close to zero (similarly to BZV). A similar behaviour is shown by the Fig. 2b for NSE. It should be noted that both NSE and NB are almost constant as a function of Z_{dr}.

Similar results are found for the LBA and MAP datasets. For the LBA dataset experimental χ_{pp} presents on average NB ~ 0, whereas NB of PB, BC, BZV, and THBRS is 3.6%, 0.2%, 1.5%, and 0.8%, respectively. The NB of (2) does not present any variability with Z_{dr}, denoting the good performance of the polynomial over the entire interval of the equivalent volume diameter.

For the MAP dataset, (3) presents a performance very close to the BC relation. The average NB over the entire Z_{dr} range variability is practically zero for both (3) and BC, whereas it is -3.5%, 1.7% and 0.9% for PB, BZV and THBRS, respectively. For NSE the performance of (3) and BC are very similar, showing lower values when compared to the other models (NSE is 4%, 2.7%, 2.3%, 2.1% and 2.0% for PB, BZV, THBRS, BC and (3), respectively).

A thorough examination of the three fourth order polynomials in the RDSSD (Fig 2) reveals that the retrieved drop shape-size models exhibit two distinct regions with different characteristics. In the first one, for Z_{dr}<1.2 dB, the curves reveal different slopes, in particular a smooth one for TEFLUN-B and steep one for MAP and LBA. In the second region, the slopes

remain substantially similar to each other, with a slight tilt downwards. Figure 4 compares all the experimental shape-size relations with the PB, BC, THBRS, and BZV models.

In conclusion, obtained results document the degree of change of the mean drop shape-size relation governing the natural rain. Specifically, for the cases considered in this study, the variability of the drop shape-size is between the values given by the BC and BZV models.
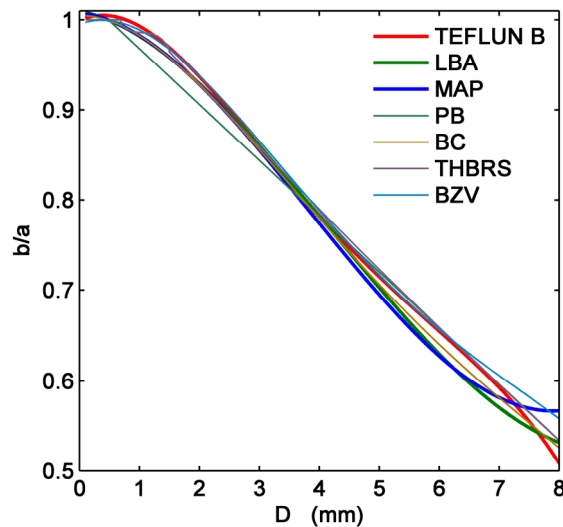

Figure 4. Shape-size relations of oblate drops as a function of equivalent volume diameter retrieved from the NCAR SPOL daasets in comparison with shape-size relations of PB, BC, BZV, and THBRS.

6. REFERENCES

Beard K. V., and C. Chuang, 1987: A new model for the equilibrium shape of raindrops. *J. Atmos. Sci.*, 44, 1509–1524.

Bechini R, Baldini L, Cremonini R, Gorgucci E, 2008: Differential reflectivity calibration for operational radars. *J. Atmos. Oceanic Technol.*, 25, 1542–1555.

Brandes, E. A., G. Zhang, and J. Vivekanandan, 2002: Experiments in rainfall estimation with a polarimetric radar in a subtropical environment. *J. Appl. Meteor.*, 41, 674–685.

Bringi, V. N. and V. Chandrasekar, 2001: Polarimetric Doppler weather radar: Principles and applications. Cambridge University Press, 648 pp.

Chandrasekar, V., S. Lim, and E. Gorgucci, 2006: Simulation of X-band rainfall observations from S-band radar data. *J. Atmos. Oceanic Technol.*, 23, 1195-1205.

Gorgucci, E., G. Scarchilli, and V. Chandrasekar, 1992: Calibration of radars using polarimetric techniques. *IEEE Trans. Geosci. Remote Sens.*, 30, 853–858.

—, —, and V. Chandrasekar, 1999: A procedure to calibrate multiparameter weather radar using properties of the rain medium. *IEEE Trans. Geosci. Remote Sens.*, 37, 269–276.

—, L. Baldini, and, V. Chandrasekar, 2006: What is the shape of raindrops? An answer from radar measurements. *J. Atmos. Sci.*, 63, 3033-3044.

—, V. Chandrasekar, and L. Baldini 2006: Can a unique model describe the raindrop shape-size relation ? A clue from polarimetric radar measurements. *J. Atmos. Oceanic Technol.*, in press.

Pruppacher, H. R. and K.V. Beard, 1970: A wind tunnel investigation of the internal circulation and shape of water drops falling at terminal velocity in air. *Quart. J. Roy. Meteor. Soc.*, 96, 247-256.

Ryzhkov, A. V., S. E. Giangrande, V. M. Melnikov, T. J. Schuur, 2005: Calibration Issues of Dual-Polarization Radar Measurements. *J. Atmos. Oceanic Technol.*, 22, 1138-1155.

Thurai, M., G. J. Huang, V. N. Bringi, W. L. Randeu and M. Schönhuber, 2007: Drop shapes, model comparisons, and calculations of polarimetric radar parameters in rain. *J. Atmos. Oceanic Technol.*, 24, 1019-1032.